

This author's accepted manuscript may be used for non-commercial purposes in accordance with [Wiley Terms and Conditions for Self-Archiving](#).

The full details of the published version of the article are as follows:

TITLE: Computed tomographic findings in 44 dogs and 10 cats with grass seed foreign bodies

AUTHORS: D. P. Vansteenkiste, K. C. L. Lee, **C. R. Lamb**

JOURNAL TITLE: Journal of Small Animal Practice

PUBLISHER: Wiley

PUBLICATION DATE: November 2014

DOI: [10.1111/jsap.12278](https://doi.org/10.1111/jsap.12278)

1 **Computed tomographic findings in 44 dogs and 10 cats with grass seed foreign bodies**

2 D.P. Vansteenkiste, K. Lee, C.R. Lamb

3 From the Department of Clinical Sciences and Services, The Royal Veterinary College,

4 University of London.

5 Address correspondence to: C.R. Lamb, Department of Clinical Sciences and Services, The

6 Royal Veterinary College, Hawkshead Lane, North Mymms, Hertfordshire AL9 7TA, U.K.

7 Email: clamb@rvc.ac.uk

8

9 Key words: cat, computed tomography, dog, foreign body, grass seed

10 Running head: CT of grass seed foreign bodies

11 **Summary**

12 Objective. To supplement recent reports of computed tomographic (CT) findings in dogs and
13 cats with grass seed foreign bodies.

14 Methods. Retrospective review of cases that had CT scan and subsequent retrieval of a grass
15 seed during the same period of hospitalisation from a site included in the scan.

16 Results. Records of 44 dogs and 10 cats were reviewed. Most were presented in the months
17 July-December. Median duration of clinical signs was 4 weeks (range 2 days- 2years). The
18 most frequent clinical signs were soft tissue swelling (30% cases), coughing (28%), sneezing
19 (28%) and discharge (26%). Grass seeds were retrieved from the thorax (35% cases), nasal
20 cavity (31%), ear (7%), other sites in the head and neck (22%), sublumbar muscles (2%) and
21 pelvic limb (2%). The grass seed was visible in CT images in 10 (19%) cases. Secondary
22 lesions were visible in CT images of 52 (96%) cases, including collection of exudate (37%),
23 abscess (24%), enlarged lymph nodes (22%) and pulmonary consolidation (20%). CT images
24 appeared normal in 4% animals.

25 Conclusions. Grass seeds within the respiratory tract are frequently visible in CT images, but
26 in general CT appears to be more useful for localisation of secondary lesions than as a
27 method of definite diagnosis.

28 **Introduction**

29 Grass seed migration is a well-recognised problem in dogs and cats (Brennan and Ihrke 1983,
30 Crha et al. 2003). Grass spikes, spikelets and individual florets (which contain the grass seed)
31 may be retrieved from many sites, including the ears, eyes, nose, brain, vertebral canal,
32 thorax, abdomen, retroperitoneum, subcutaneous tissues and feet (Johnston and Summers
33 1971, Brennan and Ihrke 1983, Lotti and Niebauer 1992, Aronson and Gregory 1995, Frendin
34 1997, Frendin et al. 1999, Demetroiu et al. 2002, Rooney and Monnet 2002, Crha et al. 2003,
35 Hopper et al. 2004, Dennis et al. 2005, Granger et al. 2007, Dembovska et al. 2009, Baglietto
36 et al. 2011, Weinmann et al. 2012, Cerquetella et al. 2013, Marvel and MacPhail 2013,
37 Bouabdallah et al. 2014, Linon et al. 2014, Tinterrud et al. 2014). In many cases, septic
38 inflammation occurs as a result of infection by various bacteria that are carried by the seed,
39 particularly *Actinomyces* or *Nocardia* spp. (Johnston and Summers 1971, Brennan and Ihrke
40 1983, Frendin 1997). Inhaled grass seeds may pass down the trachea and bronchi, migrate
41 into the pleural cavity and by following the diaphragm can reach the retroperitoneum and
42 lumbar vertebrae (Johnston and Summers 1971, Frendin et al. 1999, Marvel and MacPhail
43 2013, Bouabdallah et al. 2014). Migrating grass seeds in the urinary tract may cause
44 obstruction or act as a nidus for calculus formation (Savet et al. 2008, Cherbinksy et al. 2010,
45 Del Angel-Caraza et al. 2011).

46 Retrieval of grass seeds can be difficult because their routes of migration are unpredictable,
47 they can be deeply embedded in dense fibrous tissue, and embedded fragments may be small
48 and hard to recognise (Frendin et al. 1999). Plant material that is flimsy and/or impregnated
49 with water may be indistinguishable radiographically from adjacent soft tissues, hence
50 radiographic signs in affected animals usually represent inflammatory lesions rather than the
51 foreign body itself (Johnston and Summers 1971, Frendin et al. 1999, Demetroiu et al. 2002,
52 Schultz and Zwingenberger 2008, Baglietto et al. 2011, Tinterud et al. 2014).

53 Ultrasonographic diagnosis of a grass seed foreign body is possible (Armbrust et al. 2003,
54 Gnudi et al. 2005, Schultz and Zwingenberger 2008, Cherbinsky et al. 2010, Attanasi et al.
55 2011) and ultrasound guidance has been used to directly retrieve grass seeds from superficial
56 abscesses (Staudte et al. 2004, Della Santa et al. 2008); however, applications of
57 ultrasonography are limited by access. For example, a grass seed within the respiratory tract
58 is unlikely to be detectable because of reflection of the ultrasound beam by surrounding air.

59 Recent reports have described the computed tomographic (CT) findings associated with grass
60 seed migration in dogs and cats (Schultz and Zwingenberger 2008, Hinken et al. 2010,
61 Attanasi et al. 2011, Baglietto et al. 2011, Bouabdallah et al. 2014). CT enabled identification
62 of the grass seed responsible for clinical signs in 2/24 (8%) dogs (Attanasi et al. 2011), 4/14
63 (29%) animals (Schultz and Zwingenberger 2008) and 4/11 (36%) animals (Bouabdallah et
64 al. 2014). Grass seeds are reported to appear in CT images as foci of soft-tissue attenuation in
65 air-containing structures, as elongated gas-containing foci in soft tissues or as slightly
66 hyperattenuating foci within soft tissues (Schultz and Zwingenberger 2008, Attanasi et al.
67 2011, Bouabdallah et al. 2014). CT images may also reveal abnormalities that can be used to
68 estimate the position of a foreign body in patients in which it is not directly visualised. These
69 abnormalities include signs of soft tissue inflammation, cavitary lesions, tracts and
70 pulmonary consolidation (Schultz and Zwingenberger 2008, Attanasi et al. 2011, Baglietto et
71 al. 2011, Bouabdallah et al. 2014).

72 The aim of the present study was to supplement existing reports by describing in detail the
73 CT findings associated with grass seed migration in a larger series of cases.

74

75 **Materials and Methods**

76 Electronic case records in the period between August 2004 and October 2013 were searched
77 for patients that had CT imaging and subsequent retrieval of an intact grass seed or grass seed
78 fragment identified by the attending clinician during the same period of hospitalisation from a
79 site included in the CT. For all cases that satisfied these criteria, history, clinical findings,
80 radiological reports and CT images were reviewed.

81 CT scans prior to August 2009 were performed using a single slice helical CT scanner
82 (PQ5000, Universal Medical Systems, Solon, Ohio). CT scans after this date were performed
83 using a 16-slice CT helical scanner (Mx8000 IDT, Philips, Best, The Netherlands). All CT
84 scans were performed with patients under general anaesthesia. Thoracic CT scans were
85 performed during temporary apnoea induced by hyperventilation. CT machine settings varied
86 according to the anatomical region of interest. Nasal scans were performed using 120kVp,
87 150mAs, 1.0-1.5mm slice thickness and sharp reconstruction algorithm. CT scans of the lung
88 in dogs were performed using 120kVp, 150-250mAs, 3.0-5.0mm slice thickness and a sharp
89 reconstruction algorithm. CT scans to examine cervical soft tissues, thoracic soft tissues and
90 the abdomen in dogs were performed using 120kVp, 150-250mAs, 2.0-5.0mm slice thickness
91 and standard reconstruction algorithm. CT scans of cats were generally performed using
92 similar settings as for dogs, but with 90kVp instead of 120kVp, reduced slice thickness and a
93 smaller field of view. Matrix size was 512 x 512 and pixel size 0.3-0.6mm, depending on the
94 size of the patient. Repeat CT imaging immediately after intravenous administration of a
95 600mgI/kg bolus of Iohexol (Omnipaque, Nycomed, Oslo) was performed routinely in all
96 cases, except those having CT specifically to examine the nasal cavity.

97 For the purpose of the present study, CT images were reviewed by a Board-certified
98 radiologist with knowledge of the diagnosis and site of retrieved grass seeds. Images were
99 reviewed using various display settings: soft tissue (width 350, level 50); bone (width 2500,
100 level 500); and lung (width 2000, level -500). Adjustments to image window width and level,

101 multiplanar reconstructions, and maximum and minimum intensity slab projections were
102 made as considered necessary for review of each case. Based on localisation of a suspected
103 abscess cavity in post-contrast CT images, circular regions of interest were placed for
104 measurement of attenuation (Hounsfield units, HU) of abscess contents in pre-contrast
105 images.

106 The difference in median age of canine and feline patients was tested using the Mann-
107 Whitney test. The variation in seasonal occurrence of referrals was tested using Poisson
108 distribution. Associations between species and gender ratio and sites from which grass seeds
109 were retrieved were tested using cross-tabulation. Statistical tests were done using SPSS
110 version 19 (IBM Corporation, Chicago, Illinois). Results with $p < 0.05$ were considered
111 significant.

112

113 **Results**

114 *Patients*

115 Records of 44 dogs and 10 cats were found that satisfied the inclusion criteria (Table 1).

116 Affected dogs were significantly younger than cats ($p = 0.002$). There were 28 male dogs (17
117 neutered) and 16 female dogs (9 neutered), 6 neutered male cats and 4 neutered female cats.

118 The difference in gender ratio between dogs and cats was not significant. Canine breeds
119 included mixed breed ($n = 7$), springer spaniels ($n = 6$), Labrador retriever ($n = 5$), cocker
120 spaniel ($n = 4$), pointer ($n = 3$), Staffordshire bull terrier ($n = 3$), lhasa apso ($n = 2$) and one
121 each of Dalmatian, bull mastiff, flat-coated retriever, boxer, American bulldog, English
122 bulldog, French bulldog, Cairn terrier, Cavalier King Charles spaniel, bichon frisé, beagle,
123 Bernese mountain dog, lurcher and miniature poodle. Feline breeds included domestic
124 shorthair ($n = 6$), and one each of domestic longhair, British shorthair, Persian and Bengal.

125 Only 11 (20%) animals were admitted in the months January-June compared to 43 (80%)
126 animals admitted in July-December ($p < 0.00002$). Median duration of clinical signs referable
127 to grass seed foreign bodies was 4 weeks (range 2 days- 2 years).

128 In dogs grass seeds were found in a range of locations, whereas in cats grass seeds were
129 found predominantly in the nose (Table 1). Thoracic grass seeds were retrieved from a
130 bronchus in 14 instances (right caudal in 7, left caudal in 6, right middle in 1) from the
131 thoracic wall in 4 and from the pleural cavity in one. The method of grass seed removal was
132 surgery in 26 cases (48%), endoscopy in 22 (41%), flushing the external ear canal in four
133 (7%), ultrasound-guided aspiration in one (2%) and conjunctival flush in one (2%).

134 Overall, the most frequent clinical signs were soft tissue swelling in 16 (30%) cases,
135 coughing in 15 (28%), sneezing in 15 (28%) and discharge from an orifice or sinus in 14
136 (26%). Pyrexia was reported in 11 (20%) cases and neutrophilia ($>11.5 \times 10^9/L$) in 12 (22%)
137 cases. Only two dogs had both pyrexia and neutrophilia; both had pulmonary consolidation
138 associated with bronchial grass seeds.

139 Clinical signs associated with grass seeds were related to their anatomical location. Grass
140 seeds affecting the thorax were associated with cough in 13 (68%) cases, pyrexia in 8 (42%)
141 cases, lethargy in 5 (26%) cases, thoracic wall swelling in 4 (21%) cases, draining sinus in 3
142 (16%) cases, tachypnoea in 3 (16%) cases, enlarged regional lymph nodes in 2 (11%) cases
143 and inappetence in 2 (11%) cases. One dog that had a bronchial grass seed for approximately
144 2 years had limb pain and diffuse periosteal reactions on limb bones compatible with
145 hypertrophic osteopathy. Grass seeds in the nasal cavity were associated with sneezing in 15
146 (88%) cases, nasal discharge in 9 (53%) cases, epistaxis in 2 (12%) cases, head-shaking in 2
147 (12%), pawing or rubbing the muzzle in 2 (12%) cases and cough in 1 (6%) case. In two dogs
148 from which nasal grass seeds were retrieved, owners reported seeing their dog inhale the
149 grass seeds. Grass seeds in the ear were associated with aural pruritus in 3 (75%) cases, otitis

150 externa in 1 (25%) case, head tilt in 1 (25%) case and head shaking in 1 (25%) case. Grass
151 seeds in other sites in the head and neck were associated with a soft tissue swelling in 11
152 (92%) cases and discharge in 2 (17%) cases. The cat with a grass seed lodged in the
153 sublumbar muscles had cough, signs of lumbar pain and pyrexia. The dog with a grass seed
154 lodged in the pelvic limb had swelling and pyrexia.

155 *CT findings*

156 The grass seed was visible in CT images in 10 (19%) cases. In each instance the grass seed
157 was located in an airway (bronchus in 6 instances, nasal cavity or nasopharynx in 3 and
158 external ear canal in 1), and was visible only when using a wide CT display window suitable
159 for lung. Appearances of grass seeds varied from delicate linear structures, representing grass
160 seed fragments, elongated fusiform structures representing individual intact florets, or an
161 oblong cluster of soft tissue and gas foci representing part of the spike or spikelet (figure 1).

162 Secondary lesions associated with grass seeds were visible in 52 (96%) cases and CT images
163 appeared normal in 2 (4%) cases. CT findings varied with anatomical site of grass seeds. CT
164 images of the nasal cavity had signs of exudate in 15 (88%) cases, localised loss of turbinate
165 structure in 4 (24%) cases (figure 2), a linear intraluminal inclusion compatible with the
166 retrieved grass seed in 3 (18%) cases and appeared normal in one (6%) case. CT images of
167 the ears had thickened lining of the external ear canal in 2 (50%) cases, a linear intraluminal
168 inclusion compatible with retrieved grass seed in 1 (25%) case, signs of exudate in the
169 tympanic cavity in 1 (25%) case, para-aural soft tissue swelling in 1 (25%) case, and enlarged
170 ipsilateral medial retropharyngeal lymph node in one (25%) case. CT images of other sites in
171 the head and neck had signs of cavitory lesions compatible with abscesses in 9 (75%) cases,
172 soft tissue swelling in 7 (58%) cases, enlarged regional lymph nodes in 7 (58%) cases and
173 appeared normal in one (8%) case. Gas pockets were evident in 3 (33%) suspected abscesses.

174 CT images of the thorax had signs of focal or multifocal pulmonary consolidation in 11
175 (58%) cases (figure 3), a linear intraluminal inclusion compatible with retrieved grass seed in
176 6 (32%) cases, pleural fluid in 4 (21%) cases, pleural gas in 3 (16%) cases, thickening of soft
177 tissues in the thoracic wall in 3 (16%) cases, pulmonary cavitory mass in 2 (11%) cases,
178 enlarged thoracic lymph nodes in 2 (11%) cases and overinflation of the affected lung lobe in
179 1 (5%) case. In 4 animals with pleural fluid, attenuation of fluid ranged from 19–28 HU.
180 Irregular masses within the pleural cavity were evident in post-contrast CT images in 2
181 animals with pleural fluid (figure 4). At surgery, these masses were adherent to pleural
182 surfaces and appeared to be composed of granulation tissue and fibrin. All animals with
183 pleural fluid or gas had peripheral pulmonary consolidation. In one dog a focal defect was
184 observed affecting the visceral pleura of the right caudal lobe at the exact site from which a
185 grass seed was subsequently retrieved surgically (figure 5).

186 In the cat with a grass seed lodged in the sublumbar muscles, CT images had signs of focal
187 consolidation affecting the tip of the left caudal lung lobe and a focal cavitory lesion
188 compatible with an abscess on the left aspect of the cranial abdominal aorta. In the dog with a
189 grass seed lodged in the pelvic limb CT images had signs of two subcutaneous cavitory
190 swellings compatible with abscesses containing gas, stranding of sub-cutaneous fat and
191 enlarged ipsilateral medial iliac and superficial inguinal lymph nodes.

192 A total of 14 surgically-confirmed abscesses were identified in CT images of animals in this
193 series, each containing a grass seed or fragment; however, grass seeds were not identified in
194 CT images in any abscess. Abscess cavities were clearly defined only in post-contrast CT
195 images in which the wall of the abscess accumulated contrast medium (figure 6). Wall
196 thickness in eight abscesses in which it was relatively regular was 2-5mm; in the remaining
197 abscesses the wall was uneven in thickness or had ill-defined margins with surrounding
198 tissues, which prevented accurate measurement. Ten abscesses were considered unicameral

199 and four multicameral. Median attenuation of abscess cavities was 30 HU (range 5-60 HU).
200 Stranding of adjacent fat was evident in CT images in 10/12 (83%) abscesses in locations
201 with adjacent fat. Enlarged regional lymph nodes were evident in 8/13 (62%) animals with
202 abscesses.

203

204 **Discussion**

205 Grass seed foreign bodies may affect animals of any age and breed. It is unclear why affected
206 cats should be significantly older than affected dogs in the present series. The inclusion of six
207 retrievers and six springer spaniels in the present series is consistent with previous reports in
208 which hunting dogs have been well represented (Lotti and Niebauer 1992, Schultz and
209 Zwingenberger 2008, Cerquetella et al. 2013).

210 Schultz and Zwingenberger (2008) noted a seasonal variation in the occurrence of
211 intrathoracic grass seed foreign bodies with the majority of patients presenting in the spring
212 or summer. In the present series, a significant majority of patients were referred during the
213 second half of the year, which likely reflects animals encountering grass seeds predominantly
214 during the summer and developing signs within the next few weeks or months. In the present
215 series, the median duration of clinical signs prior to referral was 4 weeks. A prolonged period
216 without signs or occurrence of low grade, non-specific signs will tend to delay referral and
217 obscure any seasonal variation.

218 Clinical signs associated with grass seeds were related to their anatomical location. Systemic
219 signs, including pyrexia and neutrophilia, were infrequent in the present series. Pyrexia and
220 neutrophilia occurred concurrently only in two dogs with bronchial grass seeds and
221 pulmonary consolidation. Neutrophilia was observed in 17/26 (65%) dogs with intrathoracic
222 grass seeds in a previous report (Schultz and Zwingenberger 2008). Site of grass seed

223 lodgement, degree of inflammation, nature of any secondary infection, chronicity and
224 treatments administered by veterinarians prior to referral are all likely to affect the possibility
225 of pyrexia and neutrophilia in these cases.

226 Bronchial grass seed foreign bodies were found in approximately equal numbers in the right
227 and left caudal bronchi in the present series. This distribution is more even than observed in
228 previous reports in which the majority of bronchial grass seeds were found on the right,
229 mainly in the right caudal and accessory lobar bronchi (Brownlie 1990, Weinmann et al.
230 2012, Cerquetella et al. 2013). In an individual patient, it may not be possible to predict the
231 site of a bronchial foreign body from the imaging findings. Even when using CT, many grass
232 seed foreign bodies will not be visualised. Conversely, CT lesions are liable to occur at sites
233 without a grass seed, for example because the grass seed has already migrated to another site
234 or because of redistribution of exudate within the bronchial tree. These considerations
235 necessitate endoscopy of the entire bronchial tree in patients with suspected grass seed
236 (Cerquetella et al. 2013).

237 All grass seeds visualised directly in CT images in the present study were in the respiratory
238 tract or were surrounded by air. Contrary to previous reports, grass seeds in CT images
239 appearing as elongated gas-containing foci or hyperattenuating foci within soft tissues were
240 not recognised (Schultz and Zwingenberger 2008, Attanasi et al. 2011, Bouabdallah et al.
241 2014). Similarly, tracts in CT images representing migration paths of the grass seeds were not
242 recognised (Schultz and Zwingenberger 2008), although the route of a migrating grass seed
243 could be deduced in some cases from the spatial relationship of lesions, for example in the cat
244 with sublumbar abscess in which there was a focus of pulmonary consolidation immediately
245 cranial to the abdominal lesion. As reported previously, CT appears to be useful mainly as a
246 method for localising sites of lesions responsible for clinical signs and as a guide for
247 ultrasonography (Attanasi et al. 2011) or exploratory surgery (Bouabdallah et al. 2014).

248 Compared to CT using scanners with a single detector row, multi-detector CT provides
249 increased spatial resolution by use of thinner slices and faster scan times (Flohr et al. 2005).

250 Abscesses associated with grass seed foreign bodies had a range of CT features that reflected
251 varying degrees of encapsulation. The abscess wall was depicted most clearly in post-contrast
252 CT images (Hinken et al. 2010). The appearance of the abscess wall varied from regular, thin
253 (2mm) and well-defined, to irregular with ill-defined margins that merged with surrounding
254 tissues, frequently with stranding of adjacent fat. Fat stranding refers to an abnormal
255 increased attenuation in fat, which occurs as a result of oedema and engorgement of
256 lymphatic vessels (Thornton et al. 2011). In dogs with abscesses, fat stranding probably
257 represents varying combinations of secondary oedema and cellulitis.

258 This series, in which grass seeds were retrieved following CT and predominantly from the
259 respiratory tract, likely under-represents anatomical sites from which retrieval does not
260 usually require CT, such as the external ears, or where retrieval is more difficult, such as
261 from the sublumbar muscles. During the review of medical records, numerous examples of
262 dogs with abscesses in the cervical region or abdomen (including the sublumbar muscles)
263 were found in which a migrating foreign body was suspected clinically to be the underlying
264 cause, but was not proven. Grass seeds can be difficult to identify even at open surgery and
265 diagnosis of grass seed may depend on histopathological examination of resected
266 pyogranulomatous tissues (Frendin 1997, Rouabdallah et al. 2013, Trinterud et al. 2014).

267 Nidus removal is considered the optimal surgical technique for cases with suspected foreign
268 body (Amalsadvala and Swaim 2006), but it requires an accurate pre-operative method of
269 identifying grass seeds. On the basis of this and other recent reports, CT does not satisfy that
270 requirement, although CT and ultrasonography in combination might (Attanasi et al. 2011).

271 Table 1. Summary of patients with grass seed foreign bodies

272

	Dogs	Cats	p
n	44	10	
Median (range) age	3y (3m-11y)	8y (2-15y)	0.002
Males:Females	28:16	6:4	0.1
Sites of grass seeds			
Nasal cavity	9 (21%)	8 (80%)	0.006
Ear	4 (9%)	0	
Other head and neck sites	12 (27%)	0	
Thorax	18 (41%)	1 (10%)	
Abdomen	0	1 (10%)	
Pelvic limb	1 (2%)	0	

273

274

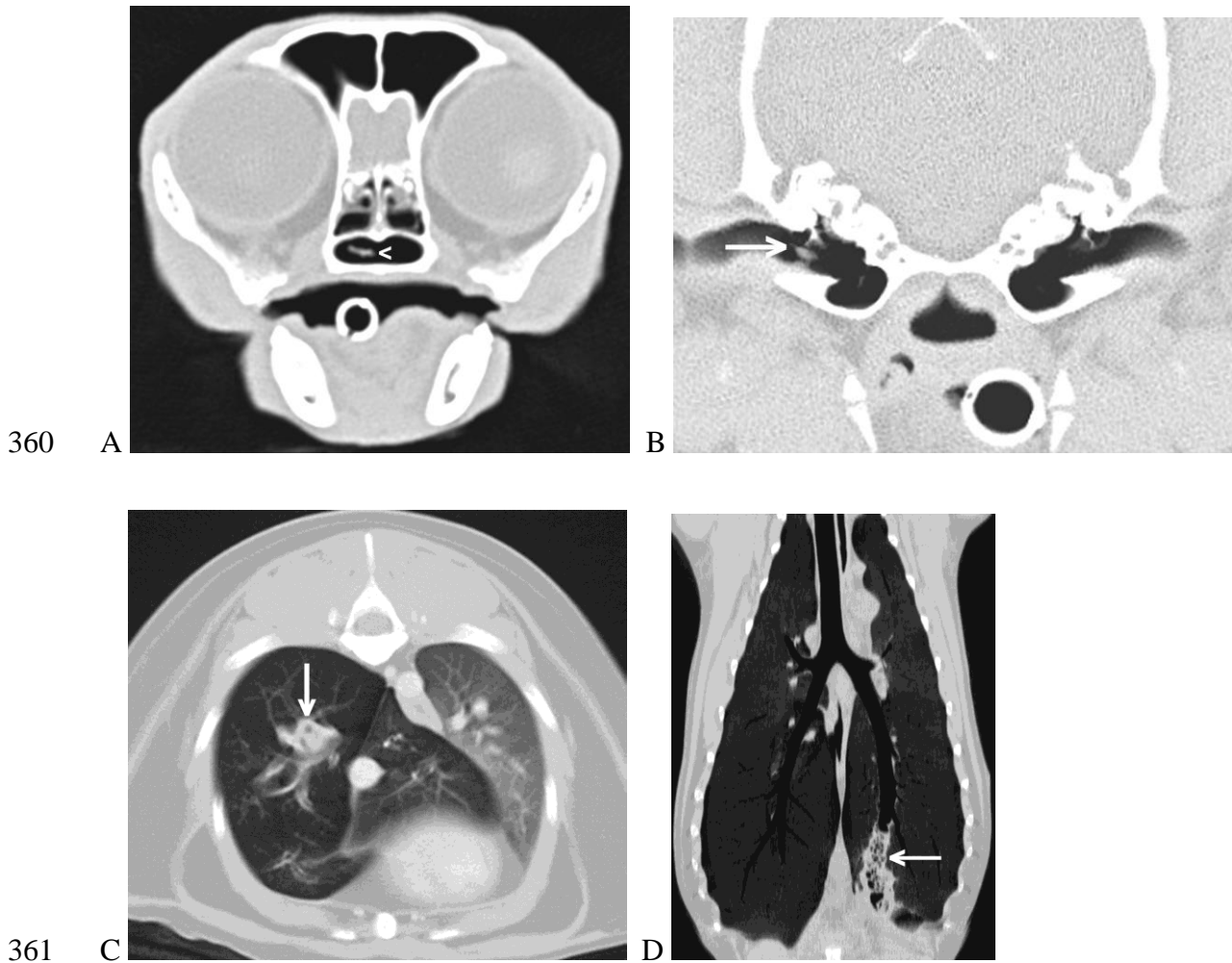
275 **References**

- 276 Amalsadvala, T. and Swaim, S.F. (2006) Management of hard-to-heal wounds. *Veterinary*
277 *Clinics of North America: Small Animal Practice* 36, 693-711
- 278 Armbrust, L.J., Biller, D.S., Radlinsky, M.G. et al. (2003) Ultrasonographic diagnosis of
279 foreign bodies associated with chronic draining tracts and abscesses in dogs. *Veterinary*
280 *Radiology and Ultrasound* 44, 66-70
- 281 Aronson, L.R. and Gregory, C.R. (1995) Infectious pericardial-effusion in 5 dogs. *Veterinary*
282 *Surgery* 24, 402-407
- 283 Attanasi, G., Laganga, P., Rossi, F. et al. (2011) Use of ultrasonography and CT in the
284 diagnosis and treatment of plant foreign bodies in 56 dogs. *Veterinaria* 25, 25-30
- 285 Baglietto, M., Cloquell, A., Monteagudo, S. et al. (2011) Spinal epidural empyema associated
286 with paravertebral and sublumbar abscesses in two dogs. Diagnosis with computed
287 tomography and myelography. *Clinica Veterinaria De Pequenos Animales* 31, 85-90
- 288 Bouabdallah, R., Moissonnier, P., Delisle, F. et al. (2014) Use of preoperative computed
289 tomography for surgical treatment of recurrent draining tracts. *Journal of Small Animal*
290 *Practice* 55, 89–94
- 291 Brennan, K. E. and Ihrke P. J. (1983) Grass awn migration in dogs and cats - a retrospective
292 study of 182 cases. *Journal of the American Veterinary Medical Association* 182, 1201-
293 1204
- 294 Brownlie, S. E. (1990) A retrospective study of diagnosis in 109 cases of canine lower
295 respiratory disease. *Journal of Small Animal Practice* 31, 371–376
- 296 Cerquetella, M., Laus, F., Paggi, E. et al. (2013) Bronchial vegetal foreign bodies in the dog -
297 localization in 47 cases. *Journal of Veterinary Medical Science* 75, 959-962

- 298 Cherbinsky, O., Westropp J., Tinga, S. et al. (2010) Ultrasonographic features of grass awns
299 in the urinary bladder. *Veterinary Radiology and Ultrasound* 51, 462-465
- 300 Crha, M., Konvalinova, J., Fichtel, T. et al. (2003) Migration of grass awn in dogs: A
301 retrospective study of 140 cases. *Kleintierpraxis* 48, 427-433
- 302 Del Angel-Caraza, J., Perez-Garcia, C.C., Bende, B. et al. (2011) Mouse barley awn
303 (*Hordeum murinum*) migration induced cystolithiasis in 2 male dogs. *Canadian*
304 *Veterinary Journal* 52, 67-69
- 305 Della Santa, D., Rossi, F., Carlucci, F. et al. (2008) Ultrasound-guided retrieval of plant
306 awns. *Veterinary Radiology and Ultrasound* 49, 484-486
- 307 Dembovska, K., Tepla, V., Fichtel, T. (2009) Migrating plant foreign body in the pyometra of
308 a bitch. *Kleintierpraxis* 54, 97-100
- 309 Demetriou, J.L., Foale R.D., Ladlow, J. et al. (2002) Canine and feline pyothorax: a
310 retrospective study of 50 cases in the UK and Ireland. *Journal of Small Animal Practice*
311 43, 388-394
- 312 Dennis, M.M., Pearce, L.K., Norrdin, R.W. et al. (2005) Bacterial meningoencephalitis and
313 ventriculitis due to migrating plant foreign bodies in three dogs. *Veterinary Pathology*
314 42, 840-844
- 315 Flohr, T.G., Schaller, S., Stierstorfer, K. et al. (2005) Multi-detector row CT systems and
316 image-reconstruction techniques . *Radiology* 235, 756-773
- 317 Frenkin, J. (1997) Pyogranulomatous pleuritis with empyema in hunting dogs. *Journal of*
318 *Veterinary Medicine Series a-Physiology Pathology Clinical Medicine* 44, 167-178
- 319 Frenkin, J., Funkquist, B., Hansson, K. et al. (1999) Diagnostic imaging of foreign body
320 reactions in dogs with diffuse back pain. *Journal of Small Animal Practice* 40, 278-285

- 321 Gnudi, G., Volta, A., Bonazzi, M. et al. (2005) Ultrasonographic features of grass awn
322 migration in the dog. *Veterinary Radiology and Ultrasound* 46, 423-426
- 323 Granger, N., Hidalgo, A., Leperlier, D. et al. (2007). Successful treatment of cervical spinal
324 epidural empyema secondary to grass awn migration in a cat. *Journal of Feline
325 Medicine and Surgery* 9, 340-345
- 326 Hinken, K., Kaiser, S., Hinken, M. (2010) Computed tomographic imaging of plant foreign
327 bodies associated with oropharyngeal injuries. *Kleintierpraxis* 55, 5-11
- 328 Hopper, B. J., Lester, N. V., Irwin, P.J. et al. (2004) Imaging diagnosis: Pneumothorax and
329 focal peritonitis in a dog due to migration of an inhaled grass awn. *Veterinary
330 Radiology and Ultrasound* 45, 136-138
- 331 Johnston, D.E. and Summers, B.A. (1971) Osteomyelitis of the lumbar vertebrae in dogs
332 caused by grass-seed foreign bodies. *Australian Veterinary Journal* 47, 289-294
- 333 Linon, E., Geissbühler, U., Karli, P. et al. (2014) Atlantoaxial epidural abscess secondary to
334 grass awn migration in a dog. *Veterinary and Comparative Orthopaedics and
335 Traumatology* 27,155-158
- 336 Lotti, U, and Niebauer, G.W. (1992) Tracheobronchial foreign-bodies of plant-origin in 153
337 hunting dogs. *Compendium on Continuing Education for the Practicing Veterinarian*
338 14, 900-905
- 339 Marvel, S. J. and MacPhail, C. M. (2013) Retroperitoneal abscesses in seven dogs. *Journal of
340 the American Animal Hospital Association* 49, 378-384
- 341 Rooney, M. B. and Monnet, E. (2002) Medical and surgical treatment of pyothorax in dogs:
342 26 cases (1991-2001). *Journal of the American Veterinary Medical Association* 221,
343 86-92

- 344 Savet, A., Goy-Thollot, I. and Carozzo, C. (2008) Hydro-ureter and hydronephrosis
345 secondary to migration of a grass awn. *Point Veterinaire* 39, 63-66
- 346 Schultz, R.M. and Zwingenberger, A. (2008) Radiographic, computed tomographic, and
347 ultrasonographic findings with migrating intrathoracic grass awns in dogs and cats.
348 *Veterinary Radiology and Ultrasound* 49, 249-255
- 349 Staudte, K.L., Hopper, B.J., Gibson, N.R. et al. (2004) Use of ultrasonography to facilitate
350 surgical removal of non-enteric foreign bodies in 17 dogs. *Journal of Small Animal*
351 *Practice* 45, 395-400
- 352 Thornton, E., Mendiratta-Lala, M., Siewert, B., et al. (2011) Patterns of fat stranding.
353 *American Journal of Roentgenology* 197, W1-W14
- 354 Trinterud, T., Nelissen, P., Caine, A.R. et al. (2014) Mediastinectomy for management of
355 chronic pyogranulomatous pleural disease in dogs. *Veterinary Record*. doi:
356 10.1136/vr.101932
- 357 Weinmann, T., Neiger, R. and Stengel, C. (2012) Endoscopic removal of tracheobronchial
358 foreign bodies: 27 dogs and 3 cats (2005-2011). *Kleintierpraxis* 57, 521-527

359 **Legends**

362 Figure 1. Examples of CT images showing grass seed foreign bodies. All images are
 363 displayed using a lung window (width 2000, level -500). A) Grass seed fragment in the
 364 nasopharynx of a cat (arrowhead), B) individual grass floret (4.5 x 1.5mm) in the external ear
 365 canal of a dog (arrow), C) portion of grass spikelet (diameter 7mm) in the dilated right caudal
 366 lobar bronchus of a cat (arrow). Note that the right caudal and accessory lobes are
 367 overinflated as a result of the partial bronchial obstruction caused by the foreign material. D)
 368 Portion of grass spike (36 x 12mm) in the left caudal bronchus of a dog (arrow).

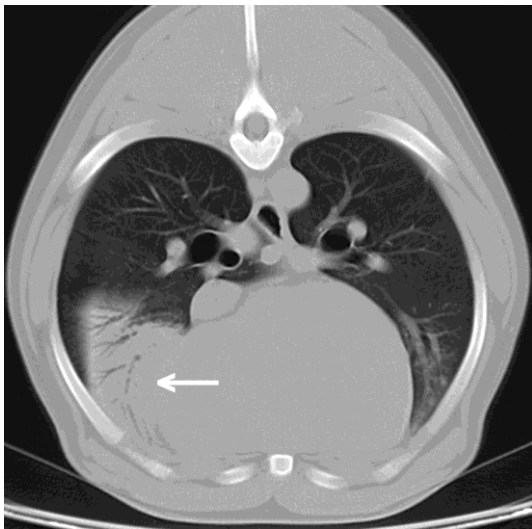
369



370

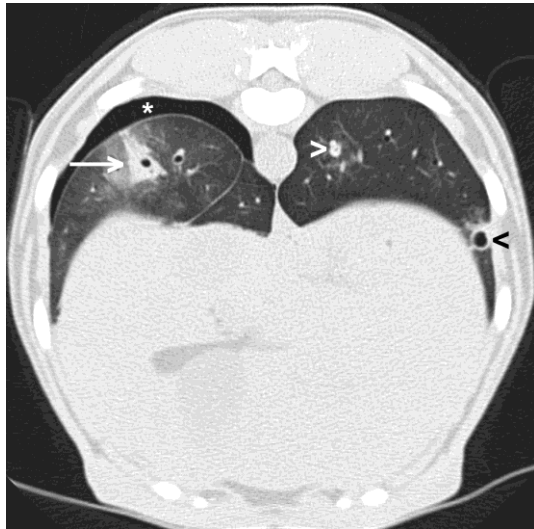
371 Figure 2. CT image (lung window, width 2000, level -500) showing localised turbinate loss
 372 (arrow) and accumulation of exudate (*) in the right nasal cavity of a dog from which a grass
 373 seed was retrieved.

374

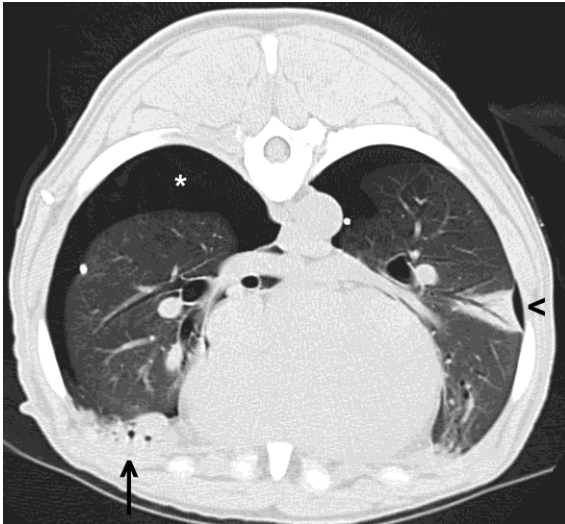


375

A



B



376 C

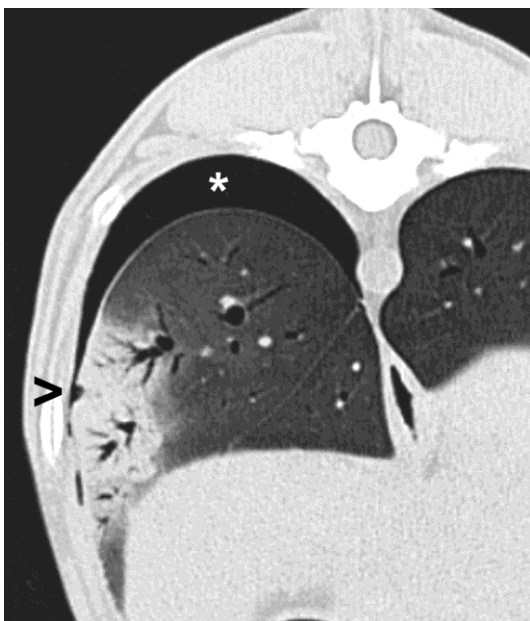
377 Figure 3. Examples of CT images (lung window, width 2000, level -500) showing pulmonary
 378 lesions associated with migrating grass seeds. A) lobar consolidation affecting only the right
 379 middle lobe (arrow) in a dog from which a grass seed was found following lobectomy. B)
 380 Multifocal lesions including a cavitary pulmonary lesion (black arrowhead), bronchial
 381 obstruction (white arrowhead) and localised consolidation in a dog in which a grass seed was
 382 retrieved endoscopically from the left caudal lobe. There is also a small volume
 383 pneumothorax on the right (*). C) Localised segmental consolidation of a portion of the left
 384 caudal lobe (arrowhead) in a dog from which two grass seeds were retrieved from the pleural
 385 cavity. There is also collapse of the tip of the right middle lobe (arrow) and pneumothorax
 386 (*). Bilateral pleural drainage tubes are present.

387



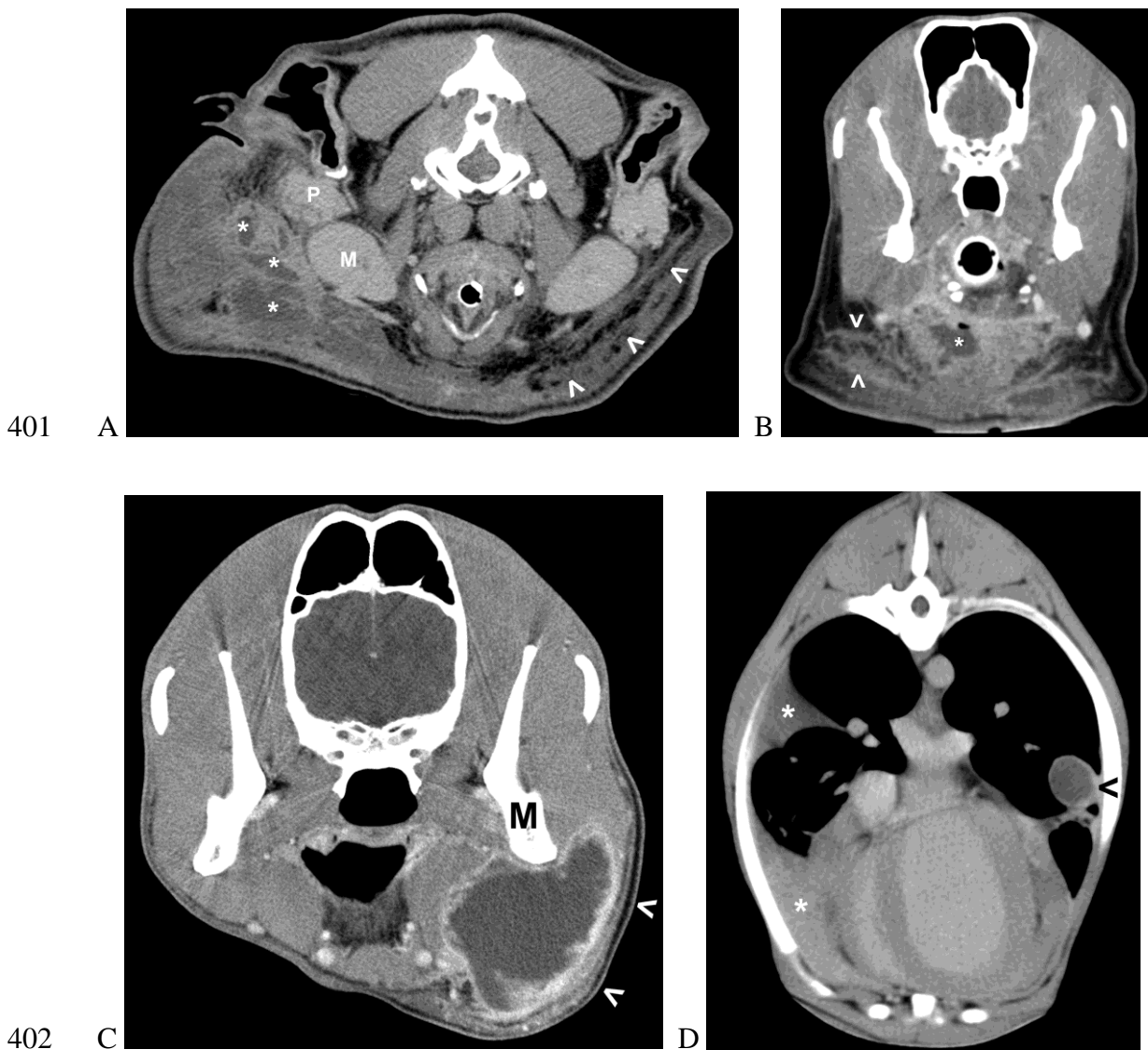
389 Figure 4. Examples of post-contrast CT images (soft tissue window, width 350, level 50)
 390 showing pleural masses in a dog with chronic pleuritis associated with grass seed foreign
 391 bodies. Transverse images through the cranial thorax (A) and costophrenic angle (B) showing
 392 pleural fluid (*) containing irregular soft tissue masses (arrowheads). Dots in B indicate the
 393 border of the liver (L).

394



396 Figure 5. CT image (lung window, width 2000, level -500) of a dog with a focal defect in the
 397 visceral pleural surface of the right caudal lobe (arrowhead). The lung adjacent to defect is
 398 consolidated and there is a small volume pneumothorax (*). At thoracotomy, a grass seed was
 399 found protruding from this defect.

400



403 Figure 6. Examples of post-contrast CT images showing features of abscesses associated with
 404 grass seed foreign bodies in dogs. All images are displayed using a soft tissue window (width
 405 350, level 50). A) Abscess comprising multiple small cavities (*) on the ventrolateral aspect
 406 of the parotid (P) and mandibular (M) salivary glands. Borders of abscess are ill-defined and

407 the lesion spreads across the ventral midline, causing stranding of sub-cutaneous fat (white
408 arrowheads), which may reflect oedema and/or inflammation. B) Abscess with a single
409 irregular cavity (*) containing a small gas bubble on the ventral aspect of the tongue. The
410 wall of the abscess appears thick and irregular. Stranding of fat (white arrowheads) is evident.
411 C) Abscess with single large cavity and well-defined, relatively regular thin wall ventral to
412 the left ramus of the mandible (M). Layer of adjacent sub-cutaneous fat appears normal
413 (white arrowheads). D) pulmonary abscess with thin regular wall (black arrowhead). This dog
414 also has pleural fluid (*).